

# Chapter 10

## Single Atom Catalysts for Environmental Remediation



Jieming Yuan and Xingmao Ma

**Abstract** Single-atom catalysts (SACs) represent an advanced class of catalysts that contain well-dispersed metal atoms on a support material. Recent studies have demonstrated the enormous potential of SACs in environmental applications. In addition to the metal atoms, the supporting material also plays an important role in the catalytic properties of SACs. The most commonly employed support material for SACs in environmental applications is the nitrogen-doped carbon due to its active chemoelectrical property, adjustable surface functional groups, porous structure, and eco-friendly nature. In environmental applications, SACs are mostly used as an activator of hydrogen peroxide, peroxymonosulfate and peroxydisulfate, extending the reaction pH limitation from less than 4.0 to a wider range of 4.0–10.0 and generating highly reactive radicals. This chapter briefly discussed the common characterization technics of SACs, the role of supporting materials and focused primarily on the activation mechanisms of common oxidants by SACs. At the end, research gaps and future needs are discussed. Overall, the unique properties and exceptional catalytic performance of SACs offer great potential for addressing the persistent environmental challenges that threaten our planet.

**Keywords** Single-atom catalyst · Organic contaminants · Environmental remediation · Carbon support

### 10.1 Introduction

The rapid progress in nanotechnology has spurred extensive applications of metal-based nanomaterials in diverse fields such as battery technology [57], sensing [2], biomedicine [12], and catalysis [14]. However, the tendency of metal nanoparticles to aggregate owing to the increased surface energy at the nano-scale [55] has impeded their broad uses and increased their cost, particularly for precious metals

---

J. Yuan · X. Ma (✉)

Zachry Department of Civil and Environmental Engineering, Texas A&M University, College Station, TX 77843, USA

e-mail: [xma@civil.tamu.edu](mailto:xma@civil.tamu.edu)

such as platinum, gold, silver, palladium, and ruthenium utilized in catalysts [59]. Consequently, considerable endeavors have been made over the last two decades to decrease the size of metal particles in catalysts from nanoparticles to single atoms [54]. The first thorough investigation of single-atom catalysts (SAC) can be traced back to 2011, when an atomically dispersed Pt/FeOx catalyst was synthesized to oxidize CO and showed a 300% higher efficiency than the bulk Pt [48]. SACs are catalysts that contain well-dispersed, catalytically active single-atom sites that are stabilized by a solid material. The catalytic process of SAC involves each metal atom in the catalyst, leading to 100% metal utilization in theory. Thus, the success of SAC can lower the cost of metal-based nanocatalysts by improving the usage of incorporated metal while reducing the risk of metal ion leakage that can negatively affect human and ecological health [12]. Most studies on SACs focus on CO oxidation, hydrogenation, and CO<sub>2</sub> reduction [7, 33, 50]. For instance, a FeOx-supported platinum single-atom catalyst was shown to be 20 times more efficient in hydrogenation than the best reported platinum-based catalyst [72]. A manganese dioxide-supported silver single-atom catalyst achieved 95.7% Faradic efficiency at  $-0.85$  V vs. RHE, resulting in stable electrochemical CO<sub>2</sub> reduction [85]. Recent studies have demonstrated that SACs have great potential in removing contaminants from water [4, 36, 87]. For example, a carbon nanotube-supported Fe SAC was reported to achieve 100% bisphenol A degradation via the activation of peroxymonosulfate (PMS) in one minute [47], while a nitrogen-rich carbon-supported Fe SAC achieved over five times faster phenol degradation than the Fe nano-catalyst via the activation of PMS [87].

While SACs have attracted a lot of attentions and many solid reviews have been available, they mostly focus on oxygen reduction reaction, hydrogenation and CO<sub>2</sub> reduction [7, 33, 50]. This book chapter aims to fill the gap by summarizing the opportunities and potential challenges of applying SACs in environmental applications. Because reviews discussing the synthesis and characterization of SAC [24, 34] have been available [7, 16, 53], this chapter will focus on the applications of SACs in water treatment. A brief introduction of characterization technology will be given, followed by a discussion on the importance of supporting materials, and the applications and mechanisms of SAC in different contaminant degradation processes. The challenges and further research need of SAC will be discussed toward the end of this work.

## 10.2 Single Atom Catalyst Characterization

### 10.2.1 *High-Angle Annular Dark-Field Scanning Transmission Electron Microscope (HAADF-STEM)*

Transmission electron microscopy (TEM) is a common technique for material characterization [56]. However, the conventional TEM is not capable of visually detecting the morphology of the single-atom sites in the catalyst due to the resolution limitation. With the rapid advancement of TEM technology in the last decades, high-angle annular dark-field scanning transmission electron microscope (HAADF-STEM) was developed based on the atomic number contrast between metals and the support materials [34]. Recently [70], a carbon black based single-atom cobalt catalyst (CoN<sub>4</sub>-CB) was synthesized and characterized with HAADF-STEM. As shown in Fig. 10.1a, the bright spots representing metal atoms can be clearly identified in the image. Energy dispersive spectroscopy (EDS) affiliated with TEM is typically used for element mapping. Figure 10.1b shows the ultra-fine distribution of N, C, and Co atoms in the catalyst [70]. Similar images were obtained by many recent single atom studies via HAADF-STEM [51, 84, 85]. However, the development of a higher resolution HAADF-STEM is still an urgent need in this field to identify every single atom active site.

### 10.2.2 *X-ray Adsorption Spectroscopy (XAS)*

XAS provides more direct information on the chemical structure and coordination environment of SACs. XAS collects the information of transmitted X-ray and the signal of scattered electrons to generate a XAS spectrum [53]. Based on the spectral region, XAS can be divided into X-ray adsorption near-edge structure spectroscopy (XANES) within the range of 30–50 eV and extended X-ray adsorption fine structure spectroscopy (EXAFS) in the range of 50–1000 eV [80]. XANES contains the information of chemical state of the targeted metal element as shown in Fig. 10.2a, indicating that Fe in the SAC has a valance state close to Fe<sub>2</sub>O<sub>3</sub>. EXAFS is capable of providing information on the coordination conditions of metal atoms in SAC, which includes the number of different coordinating species, binding energy, bond length, bond angle and so on [6, 80]. XAS can accurately capture the signal of the backscattered atoms based on the path-length criterion [6]. However, it is difficult to distinguish the backscattered atoms with the same path-length. The assistance of wavelet transform (WT) is essential to identify the specific backscattered atoms based on the information of the k position [54]. Therefore, with the help of WT, FT (Fourier transformed) EXAFS can reveal the metal coordination environment, and a further fitting can reveal the coordination structure of the targeted element as shown in Fig. 10.2b, c.

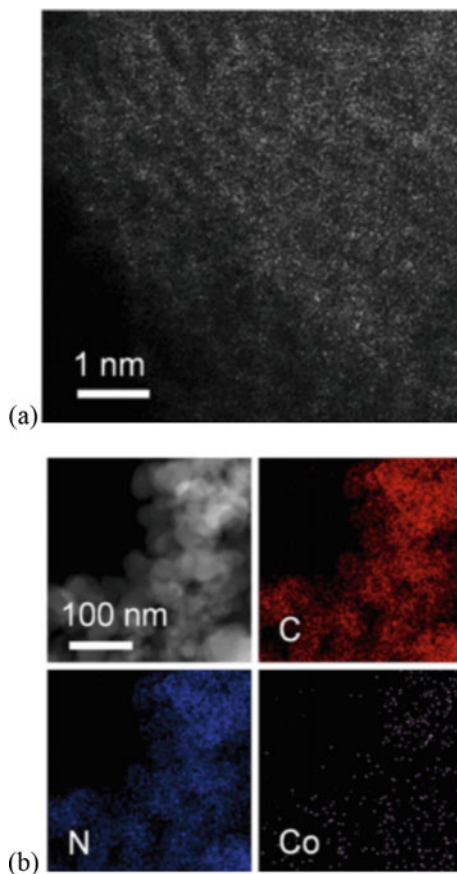


Fig. 10.1 a HAADF-STEM image of CoN<sub>4</sub>-CB, b elemental mapping of CoN<sub>4</sub>-CB [70]

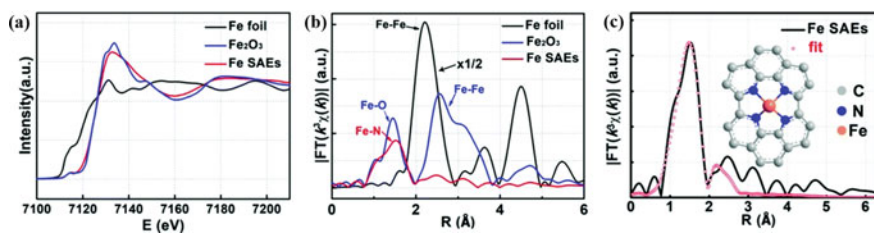


Fig. 10.2 a Normalized Fe K-edge XANES spectrum of Fe foil, Fe<sub>2</sub>O<sub>3</sub>, and Fe SAC b Fourier transformed EXAFS of Fe foil, Fe<sub>2</sub>O<sub>3</sub>, and Fe SAC c EXAFS fitting results of Fe SAC data [86]

### 10.2.3 X-ray Photoelectron Spectroscopy (XPS)

XPS is a widely used characterization technique to determine the elemental composition of SAC as well as their surface electron structure [8, 71]. XPS cannot provide direct evidence on the formation of single-atom metal active sites. However, it can measure the elemental composition of metal single atom catalysts in the parts per thousand range, revealing information on the chemical state and electronic state of metals in the catalyst that can be used to gain insight into the electronic and coordination environment [34].

### 10.2.4 Other Techniques

In addition to the above-mentioned three techniques, new characterization techniques are also emerging. For example, the *in-situ* Fourier transform infrared spectroscopy (FTIR) has been used to verify the existence of single-atom sites in carbon-based catalyst. The unchanged band position of adsorbed CO on the catalyst by *in-situ* FTIR analysis after the CO pressure increase indicates the weak interaction between CO molecules and isolated single-atom sites [48]. Therefore, the band position of CO is used as an indicator of the presence of single metal atoms. Due to the importance of metal loading rate, which affects the active metal sites on SACs, inductively coupled plasma (ICP) is a powerful tool to measure the total content of metals in the single atom metal catalyst [64]. Other more traditional methods such as X-ray diffraction (XRD), Raman spectroscopy, scanning electron microscope (SEM) have also been used in the literature for SAC characterization, however, outputs from these techniques are often used as supporting evidence of the formation of SACs [54].

## 10.3 Supporting Materials of SACs

The composition of SAC support is essential for the performance of SACs. Various materials such as TiO<sub>2</sub>, FeO<sub>x</sub>, ZnO, carbon nanotubes, graphitic nitrogen, biochar, and polymer have been used as supporting materials, and they can be mainly divided into metal-based and carbon-based [23, 25, 48]. Metal-based support materials for SACs offer several advantages such as the high thermal stability, mechanical strength, and catalytic activity [28]. However, the controlled dispersion of metal atoms on metal-based support materials can be a significant challenge, leading to the formation of metal clusters which reduce the catalytic activity and selectivity of SACs. Furthermore, metal-based support materials can be relatively expensive and the metal ion leaching problem could add new pollution to a water system, which limits their application in environmental processes. On the other hand, carbon-based materials have

high specific surface area, porosity and tunable surface, excellent electrical conductivity, and low cost [16]. Carbon-based SAC supports are highly tunable and other elements can be easily doped into the carbon structure to greatly enhance the activity of the metal single atom sites as a result of the increased impact of coordination environment on the behavior of the metal atom [66, 67]. Among all carbon-based support materials, nitrogen-doped carbon (N-doped carbon) was very popular because of the highly stable metal-nitrogen-carbon bond and the active chemoelectrical nature of N-doped carbon [7, 13]. The N-doped carbon have higher metal loading and stability than pure carbon materials because the valance shell of N atom has one more electron than C atom and it provides higher binding energy between N and metal atoms [29]. Additionally, N-doped carbon has an excellent chemoelectrical property comparable to the expensive platinum (Pt) based electrode in oxygen reduction reaction [17]. N-doping could also alter the local coordination environment of the metal single-atom sites, and greatly enhance the oxidization efficiency of carbon-based SACs [45, 46]. Thus, the incorporation of SAC into N-doped carbon becomes the most popular combination for carbon-based SACs. Additional modification of N-doped carbon support can further enhance the catalytic performance of produced SACs. For example, the extra doping of oxygen into N-doped carbon support boosted the catalytic efficiency of Fe SAC on nitrogen-rich carbon by 5.13 times [87]. In addition, fluorine doping on the N-doped carbon was reported to increase the charge density of the nearby pyridinic N, and an outstanding CO evolution rate of  $1,146 \text{ mmol g}^{-1} \text{ h}^{-1}$  was achieved by the produced nickel (Ni) SAC [18]. Metal organic framework (MOF) as a special category of N-doped carbon has been extensively applied in environmental applications, and the combination of SACs and MOFs can better exert their catalytic effects [30, 74]. The well-organized structure of MOF makes it an excellent support material for the ultrafine distribution of single atoms, and the highly designable structure can further provide a precise control of the binding location for the single-atom sties [83]. However, the cost of MOF is higher than traditional carbon-based materials, making it less cost-effective. Silica ( $\text{SiO}_2$ ) is also employed as a support material for SACs because of its remarkable thermal stability, enabling SACs to perform well in harsh environments [44]. However, the research on silica-based SACs is still limited. A better understanding of the fundamental interaction between single-atom sites and the silica support is needed.

## 10.4 Application and Mechanisms

### 10.4.1 Photocatalysis

Recent efforts in photocatalysis primarily focused on exploring advanced materials that can enhance the efficiency of photocatalysis by higher light harvesting and greater charge separation. SACs provide a promising solution to the future development in this field and the photocatalytic degradation of organic contaminants by

SAC is gaining increased attention in recent years [35, 52, 67]. To be photocatalytic, SACs usually require a semiconductor support with the semiconductor functioning as a light harvesting unit and single-atom sites providing unique electronic structures to boost the photocatalytic process [13]. The natural sunlight consists of 52% infrared light, 43% visible light, and 5% UV light. Great efforts have been made to design catalysts that can utilize visible light or even infrared light to achieve a better light utilization [60]. The incorporation of SAC into a light-harvesting support can modify the energy band structure that shifts the catalyst from UV-responsive to visible light-responsive [68]. For example, the coordination of single-atom Pt into  $g\text{-C}_3\text{N}_4$  resulted in a visible-light active photocatalyst, and the light absorption range was expanded from  $\lambda < 460$  nm for bare  $g\text{-C}_3\text{N}_4$  to the range of 460–900 nm for Pt SAC on  $g\text{-C}_3\text{N}_4$  [30]. Similar result was reported for an Ag SAC on  $g\text{-C}_3\text{N}_4$  support, and a 100% bisphenol A degradation was obtained under visible light irradiation within 60 min [65]. The metal single-atom site can enhance the separation of photo-generated electrons and holes at the interface of the semiconductor. Metal single-atom sites that are very chemoelectrical active can induce a much faster transfer of the photogenerated electrons to the targeted contaminants to reduce the electron/hole recombination [68, 77]. Photoluminescence spectroscopy was used to monitor the separation of photogenerated electrons and holes in a Pd SAC on  $g\text{-C}_3\text{N}_4$ , and a much lower charge recombination rate was found with Pd SAC/ $g\text{-C}_3\text{N}_4$  than the  $g\text{-C}_3\text{N}_4$  only [5]. Furthermore, the introduction of single-atom sites into semiconductor can also modify the structure of the catalyst to achieve a faster electron transfer. The local light-harvesting units in  $g\text{-C}_3\text{N}_4$  was found to be enhanced by the incorporation of single atom Cu into the catalyst, leading to the decrease of the charge transfer distance between light-harvesting units and thus enhanced photocatalytic activity [27]. The mechanisms of SAC enhanced photocatalysis were summarized as Fig. 10.3.

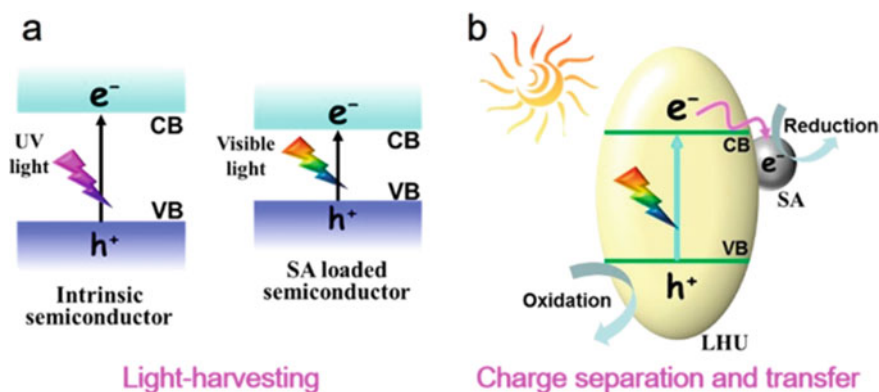


**Fig. 10.3** Schematic illustration for the roles of single-atoms in enhancing the **a** light-harvesting, **b** charge separation and transfer [13]

### 10.4.2 Activation of $H_2O_2$

Hydrogen peroxide ( $H_2O_2$ ) is a powerful oxidizing agent which is commonly used in environmental remediation [15, 41]. For example,  $H_2O_2$  could be activated by the Fenton and Fenton-like reaction to produce highly reactive  $\cdot OH$  with a redox potential of +2.8 V (vs NHE) [40] to react rapidly and non-selectively with organic contaminants [76]. Unfortunately, the classic activation of  $H_2O_2$  via Fenton reaction still suffers from many drawbacks including the requirement of low pH < 4 [61], and the leaching of iron ions into the water system [42].

SACs outperform traditional metal-loaded catalysts in the activation of  $H_2O_2$  because of the abundant active single-atom sites, relative stable structure with less metal leaching, and a wider pH window for the activation [79]. Due to the aggregation of traditional metal nanoparticles, only a small amount of active metal sites is exposed to  $H_2O_2$  [76]. In contrast, SACs can greatly enhance the activation of  $H_2O_2$  to generate  $\cdot OH$  thanks to the utmost utilization of ultrafine single-atom metal sites [21]. For example, a Copper (Cu) SAC on g- $C_3N_4$  was applied to active  $H_2O_2$ , leading to a 99.97% degradation of rhodamine B (RhB) in 5 min while less than 40% of RhB was removed by nano Cu-containing catalysts. [76]. The SAC could also result in an enhanced  $H_2O_2$  activation via stronger absorption of  $H_2O_2$  onto the single-atom sites. The M-N<sub>x</sub> sites was reported to have a strong free binding energy with  $H_2O_2$  for a rapid adsorption [79] And similar result was reported by another study that synthesized Fe, Co, Ni, Cu SAC on N-doped carbon, and found that Fe-N<sub>4</sub> has the fastest  $\cdot OH$  generation from  $H_2O_2$  activation because of the highest d-band center value [11]. Furthermore, the introduction of SAC into  $H_2O_2$  activation also extend pH limitation of the Fenton/Fenton-like reaction to a boarder pH range [61]. The SAC Cu synthesized on mesoporous silica support was reported to have an efficient activation of  $H_2O_2$  to generate  $\cdot OH$  in a wider pH range of 4.0–7.0. Additionally, the immobilization of single-atom Fe on the combination of graphitized carbon and g- $C_3N_4$  was found to have an excellent  $H_2O_2$  activation in a wide pH range of 4.0–10.0 [37]. However, the field of SACs catalyzing  $H_2O_2$  has been relatively under-studied, and it is crucial to further elucidate the catalytic mechanisms of  $H_2O_2$  activation by SACs.

### 10.4.3 Activation of Peroxymonosulfate (PMS)

Peroxymonosulfate (PMS) has been extensively researched for its ability to generate free radicals, specifically  $SO_4^{\cdot -}$ , which is effective in breaking down organic contaminants [38, 43]. The  $SO_4^{\cdot -}$  has a higher redox potential (+2.5–3.1 V vs NHE) and a longer half-life (~40  $\mu s$ ) than  $\cdot OH$  with a potential of +1.8–2.7 V (vs NHE) and half-life of 1–100 ns [10, 69]. In addition, the activation of PMS is less pH sensitive and can proceed in a wider pH range of 2.0–8.0



[54]. Thus, the application of  $\text{SO}_4^{\bullet-}$ -based reaction is more suitable in various environmental conditions. The recent introduction of SACs into the activation of PMS has garnered significant attention in the field of environmental remediation [39, 78]. SAC showed a greatly enhanced PMS activation than metal nano-particle catalysts. For instance, 33 times higher phenol degradation was observed via the PMS activation by Fe-SAC than  $\text{Fe}_3\text{O}_4$  nanoparticles [32]. Similar conclusion was drawn in another study that 100% removal of Orange II was achieved in 60 min via PMS activation by Fe-SAC while only 29.5% removal was obtained by  $\text{Fe}_3\text{O}_4$  nanoparticle and PMS [82]. The activation of PMS by SAC can be mainly divided into two pathways: radical-based and non-radical based pathways. Firstly, the PMS can be activated by SACs to generate radicals, predominantly  $\text{SO}_4^{\bullet-}$  and  $\cdot\text{OH}$  [19, 63, 75, 84]. The generation of these radicals was via the activation of PMS by a carbon supported cobalt SAC for the fast degradation of atrazine, nitrobenzene, bisphenol A, phenol and 4-chlorophenol [63]. A Cu-SAC on reduced graphene oxide system was also found to be highly effective in degrading various antibiotics including sulfafurazole, sulfamethoxazole, and meropenem in a wide range of pH, and  $\text{SO}_4^{\bullet-}$  was found as the dominant reactive species [6]. It also exhibited a remarkable mineralization capacity, with a removal efficiency of up to 99% of total organic carbon after 120 min of reaction [6]. The generation of singlet oxygen ( $^1\text{O}_2$ ) and the direct electron transfer are important non-radical pathways of PMS activation [45, 49, 78].  $^1\text{O}_2$  is highly reactive with a redox potential of +2.2 V vs NHE [88]. A graphitic carbon nitride (g- $\text{C}_3\text{N}_4$ ) supported Fe single-atom catalyst with 11.2 wt% Fe loading was reported to have a highly selective generation of 100%  $^1\text{O}_2$  by activating PMS and achieved a first order rate constant of  $1.43 \text{ min}^{-1}$  in p-chlorophenol degradation [84].

The direct electron transfer is another main degradation mechanism that a PMS-SAC complex forms upon the adsorption of PMS on SAC, and the further contact between this complex and targeted contaminant induces the direct electron transfer between them [45, 73, 78]. Direct electron transfer was identified as the dominant mechanism for the degradation of naproxen by a SA Co on N-doped carbon, while the generation of reactive oxygen species was confirmed as a minor pathway as Fig. 10.4 shows. Similar result was found in the chloroquine phosphate degradation by PMS activated by a biomass carbon-based cobalt single-atom catalyst, and 98% chloroquine phosphate was degraded in 30 min [46].

#### 10.4.4 Activation of Perdisulfate (PDS) and Sulphite

Peroxydisulphate (PDS) is another persulfate compound with a structure that includes a peroxide O–O bond length of 1.322 Å, providing higher stability compared to the asymmetric PMS. The distinctive structures of PDS and PMS contribute to differences in their activation mechanisms leading to a more active PMS activation by a wide range of carbonaceous materials and transition metal catalysts [62]. However, PDS has a lower bond dissociation energy of  $92 \text{ kJ mol}^{-1}$  compared with  $377 \text{ kJ mol}^{-1}$

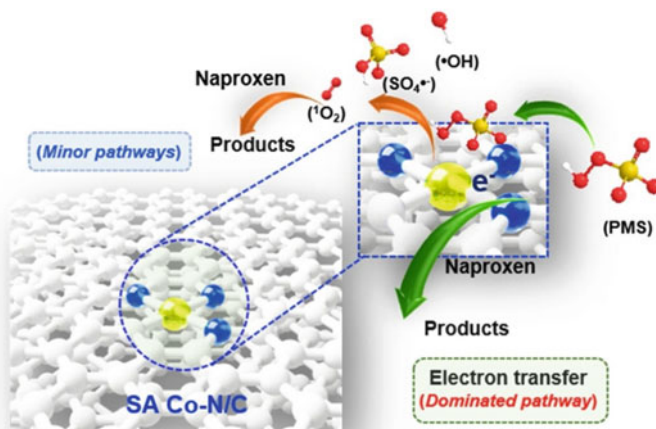


**Fig. 10.4** The activation mechanism of PMS by SA Co on N-doped carbon [49]

of PMS [3], resulting in an easier activation of PDS by energy transfer [54]. Recent advancements in catalysts have aimed to enhance PDS activation, with SACs outperforming conventional catalysts due to their highly dense and reactive single atom metal sites [20]. The activation of PDS is similar to PMS in terms of the reactive radical species. A cobalt SAC stabilized on N-doped carbon effectively activated PDS to generate  $\text{SO}_4^{\bullet-}$  to achieve a high specific activity of  $0.067 \text{ Lmin}^{-1} \text{ m}^{-2}$  for the degradation of bisphenol A [26]. Notably, instead of the activation of PDS by SAC to oxidize contaminants directly, PDS can oxidize the metals in SAC to generate high valence metals to react with pollutants. One study found the generation of Fe (V) in PDS activation by Fe (III) SAC on N-doped carbon [22]. The Fe (III) site was oxidized by the PDS via a two-electron abstraction to Fe (V) as a metastable oxidant (Fig. 10.5), which enables selective 97% degradation of 2,4-dichlorophenol in 90 min [22].

Sulphite has gained recognition as a more environmentally friendly alternative to PMS and PDS in the production of oxysulphur radicals such as  $\text{SO}_3^{\bullet-}$ ,  $\text{SO}_4^{\bullet-}$ ,

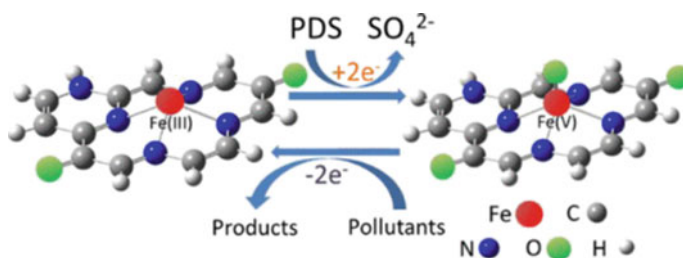


**Fig. 10.5** The generation of Fe (V) via the activation of PDS by SFe on N-doped carbon [22]

and  $\text{SO}_5^{\bullet-}$  to break down refractory organic compounds [9, 81]. Unlike PMS and PDS, sulphite has lower chronic biotoxicity and cost, leading to a more sustainable and environmentally friendly treatment process. However, the traditional transition metal-based catalyst is not able to achieve an efficient sulphite activation [54]. The introduction of SACs into sulphite activation greatly enhances this process. A Co-SAC on MOF resulted in a 2.6 times higher oxidation rate than other Co-based nanoparticles, and  $\text{SO}_4^{\bullet-}$  radical was detected as the dominant reactive species [31].  $\text{SO}_5^{\bullet-}$  radical was reported as the dominating reactive species generated by a Fe SAC supported on molybdenum disulfide, and a 90% degradation of propranolol was obtained in 30 min.

PDS and sulphite represent promising oxidizing agents in environmental remediation due to their low cost, widespread availability, and high oxidation capacity [1, 22, 31]. While PMS and  $\text{H}_2\text{O}_2$  have been extensively studied in advanced oxidation processes (AOPs), the catalytic potential of SAC in PDS and sulphite-based systems remains relatively unexplored. Therefore, the development of cost-effective and efficient SACs for PDS and sulphite activation is highly desirable.

## 10.5 Future Research Needs

The development of single atom catalysts encounters multiple challenges that must be tackled to further improve their stability and performance. The first challenge is the precise control of the uniform dispersion of single atoms on the support, which necessitates precise control over the synthesis process. The utilization of MOF as support material for SACs could be a potential solution because the highly organized structure of MOF can be easily designed to load desired single-atom sites [83]. The atomic layer deposition method can have the precise control of the distribution of the single-atom sites in the produced catalyst, however, efforts are needed to cut down the cost of this method [58]. Furthermore, optimizing interactions between single atoms and the support is necessary to ensure efficient charge transfer and catalytic activity. Doping of two or more elements simultaneously into the catalyst could be a promising method to further enhance the catalytic activity of SACs. The doping of oxygen and nitrogen into carbon support was found to result in an improved catalytic performance [87], while the double-doping of fluorine and nitrogen on carbon support was reported to increase the charge density of the produced SAC [18]. However, the scalability and cost-effectiveness of the SAC synthesis process are still at a low end. The synthesis of the SAC is still limited to lab scale due to the strict reaction conditions and the complicated synthesis method. Addressing these challenges would unlock the potential of carbon-based single atom catalysts for a boarder application in the environmental field.

## 10.6 Conclusions

In summary, SACs have shown great potential in environmental applications, particularly in water treatment. Their unique properties of high efficiency, selectivity, and 100% atom utilization have made them a promising alternative to conventional metal-based catalysts. Various studies have demonstrated the successful application of SACs in the degradation of environmental contaminants via photocatalysis or the activation of  $\text{H}_2\text{O}_2$ , PMS, PDS and sulphite, showing their excellent stability and outstanding catalytic performance. However, there are still many challenges to overcome, such as the low control of the distribution of the single-atom sites, low scalability and cost-effectiveness of the SAC synthesis process. Overall, the potential of SACs in environmental applications is enormous, and the development of SACs holds great promise for the future of sustainable and green technology in the environmental field.

## References

1. Abdelhaleem A, Chu W, Farzana S (2020) Diphenamid photodegradation using Fe (III) impregnated N-doped  $\text{TiO}_2$ /sulfite/visible LED process: influence of wastewater matrix, kinetic modeling, and toxicity evaluation. *Chemosphere* 256:127094
2. Bai J, Zhou B (2014) Titanium dioxide nanomaterials for sensor applications. *Chem Rev* 114(19):10131–10176
3. Benson SW (1978) Thermochemistry and kinetics of sulfur-containing molecules and radicals. *Chem Rev* 78(1):23–35
4. Cai S, Zuo X, Zhao H, Yang S, Chen R, Chen L, Zhang R, Ding D, Cai T (2022) Evaluation of N-doped carbon for the peroxymonosulfate activation and removal of organic contaminants from livestock wastewater and groundwater. *J Mat Chem A* 10(16):9171–9183
5. Cao S, Li H, Tong T, Chen H, Yu A, Yu J, Chen HM (2018) Single-atom engineering of directional charge transfer channels and active sites for photocatalytic hydrogen evolution. *Adv Func Mater* 28(32):1802169
6. Chen F, Wu X-L, Yang L, Chen C, Lin H, Chen J (2020) Efficient degradation and mineralization of antibiotics via heterogeneous activation of peroxymonosulfate by using graphene supported single-atom Cu catalyst. *Chem Eng J* 394:124904
7. Cheng N, Zhang L, Doyle-Davis K, Sun X (2019) Single-atom catalysts: from design to application. *Electrochem Ene Rev* 2(4):539–573
8. Ding K, Gulec A, Johnson AM, Schweitzer NM, Stucky GD, Marks LD, Stair PC (2015) Identification of active sites in CO oxidation and water-gas shift over supported Pt catalysts. *Science* 350(6257):189–192
9. Ding W, Xiao W, Huang W, Sun Q, Zheng H (2020) Sulfite activation on a silica-supported well-dispersed cobalt catalyst via an electron transfer complex path. *J Clean Prod* 257:120457
10. Duan X, Sun H, Wang S (2018) Metal-free carbocatalysis in advanced oxidation reactions. *Acc Chem Res* 51(3):678–687
11. Duan J, Zhou Y, Ren Y, Liu F, Deng P, Yang M, Ge H, Gao J, Yang J, Qin Y (2023) Effect of electronic structure over late transition-metal M1–N4 single-atom sites on hydroxyl radical-induced oxidations. *ACS Catal* 13:3308–3316
12. Fan Y, Liu S, Yi Y, Rong H, Zhang J (2021) Catalytic nanomaterials toward atomic levels for biomedical applications: from metal clusters to single-atom catalysts. *ACS Nano* 15(2):2005–2037

13. Gao C, Low J, Long R, Kong T, Zhu J, Xiong Y (2020) Heterogeneous single-atom photocatalysts: fundamentals and applications. *Chem Rev* 120(21):12175–12216
14. Gao C, Lyu F, Yin Y (2020) Encapsulated metal nanoparticles for catalysis. *Chem Rev* 121(2):834–881
15. Gao J, Yang H, Huang X, Hung S-F, Cai W, Jia C, Miao S, Chen HM, Yang X, Huang Y, Zhang T, Liu B (2020). Enabling direct H<sub>2</sub>O<sub>2</sub> production in acidic media through rational design of transition metal single atom catalyst. *Chem* 6(3):658–674. <https://doi.org/10.1016/j.chempr.2019.12.008>
16. Gawande MB, Fornasiero P, Zbořil R (2020) Carbon-based single-atom catalysts for advanced applications. *ACS Catal* 10(3):2231–2259
17. Gong K, Du F, Xia Z, Durstock M, Dai L (2009) Nitrogen-doped carbon nanotube arrays with high electrocatalytic activity for oxygen reduction. *Science* 323(5915):760–764
18. Han S-G, Ma D-D, Zhou S-H, Zhang K, Wei W-B, Du Y, Wu X-T, Xu Q, Zou R, Zhu Q-L (2021) Fluorine-tuned single-atom catalysts with dense surface Ni-N<sub>4</sub> sites on ultrathin carbon nanosheets for efficient CO<sub>2</sub> electroreduction. *Appl Catal B* 283:119591
19. Hu L, Zhang G, Liu M, Wang Q, Wang P (2018) Enhanced degradation of Bisphenol A (BPA) by peroxymonosulfate with Co<sub>3</sub>O<sub>4</sub>-Bi<sub>2</sub>O<sub>3</sub> catalyst activation: effects of pH, inorganic anions, and water matrix. *Chem Eng J* 338:300–310
20. Huang B, Wu Z, Zhou H, Li J, Zhou C, Xiong Z, Pan Z, Yao G, Lai B (2021) Recent advances in single-atom catalysts for advanced oxidation processes in water purification. *J Hazard Mater* 412:125253
21. Ji S, Jiang B, Hao H, Chen Y, Dong J, Mao Y, Zhang Z, Gao R, Chen W, Zhang R (2021) Matching the kinetics of natural enzymes with a single-atom iron nanozyme. *Nat Catal* 4(5):407–417
22. Jiang N, Xu H, Wang L, Jiang J, Zhang T (2020) Nonradical oxidation of pollutants with single-atom-Fe (III)-activated persulfate: Fe (V) being the possible intermediate oxidant. *Environ Sci Technol* 54(21):14057–14065
23. Jiao L, Wu J, Zhong H, Zhang Y, Xu W, Wu Y, Chen Y, Yan H, Zhang Q, Gu W (2020) Densely isolated FeN<sub>4</sub> sites for peroxidase mimicking. *ACS Catal* 10(11):6422–6429
24. Kottwitz M, Li Y, Wang H, Frenkel AI, Nuzzo RG (2021) Single atom catalysts: a review of characterization methods. *Chem-Method* 1(6):278–294
25. Lai W, Zhang L, Hua W, Indris S, Yan Z, Hu Z, Zhang B, Liu Y, Wang L, Liu M (2019) General  $\pi$ -electron-assisted strategy for Ir, Pt, Ru, Pd, Fe, Ni single-atom electrocatalysts with bifunctional active sites for highly efficient water splitting. *Angew Chem Int Ed* 58(34):11868–11873
26. Liang X, Wang D, Zhao Z, Li T, Chen Z, Gao Y, Hu C (2022) Engineering the low-coordinated single cobalt atom to boost persulfate activation for enhanced organic pollutant oxidation. *Appl Catal B* 303:120877
27. Li Y, Wang Z, Xia T, Ju H, Zhang K, Long R, Xu Q, Wang C, Song L, Zhu J (2016) Implementing metal-to-ligand charge transfer in organic semiconductor for improved visible-near-infrared photocatalysis. *Adv Mater* 28(32):6959–6965
28. Li X, Bi W, Zhang L, Tao S, Chu W, Zhang Q, Luo Y, Wu C, Xie Y (2016) Single-atom Pt as co-catalyst for enhanced photocatalytic H<sub>2</sub> evolution. *Adv Mater* 28(12):2427–2431
29. Li X, Rong H, Zhang J, Wang D, Li Y (2020) Modulating the local coordination environment of single-atom catalysts for enhanced catalytic performance. *Nano Res* 13(7):1842–1855
30. Li Y, Yang T, Qiu S, Lin W, Yan J, Fan S, Zhou Q (2020) Uniform N-coordinated single-atomic iron sites dispersed in porous carbon framework to activate PMS for efficient BPA degradation via high-valent iron-oxo species. *Chem Eng J* 389:124382
31. Li M, Guo Q, Xing L, Yang L, Qi T, Xu P, Zhang S, Wang L (2020) Cobalt-based metal-organic frameworks promoting magnesium sulfite oxidation with ultrahigh catalytic activity and stability. *J Colloid Interface Sci* 559:88–95
32. Li Z, Li K, Ma S, Dang B, Li Y, Fu H, Du J, Meng Q (2021) Activation of peroxymonosulfate by iron-biochar composites: Comparison of nanoscale Fe with single-atom Fe. *J Colloid Interface Sci* 582:598–609

33. Liu L, Corma A (2018) Metal catalysts for heterogeneous catalysis: from single atoms to nanoclusters and nanoparticles. *Chem Rev* 118(10):4981–5079
34. Liu Q, Zhang Z (2019) Platinum single-atom catalysts: a comparative review towards effective characterization. *Catal Sci Technol* 9(18):4821–4834
35. Liu J, Zou Y, Cruz D, Savateev A, Antonietti M, Vilé G (2021) Ligand–metal charge transfer induced via adjustment of textural properties controls the performance of single-atom catalysts during photocatalytic degradation. *ACS Appl Mater Interfaces* 13(22):25858–25867
36. Liu X, Pei Y, Cao M, Yang H, Li Y (2022) Highly dispersed copper single-atom catalysts activated peroxymonosulfate for oxytetracycline removal from water: mechanism and degradation pathway. *Chem Eng J* 450:138194
37. Ma J, Yang Q, Wen Y, Liu W (2017) Fe-g-C<sub>3</sub>N<sub>4</sub>/graphitized mesoporous carbon composite as an effective Fenton-like catalyst in a wide pH range. *Appl Catal B* 201:232–240
38. Matafonova G, Batoev V (2018) Recent advances in application of UV light-emitting diodes for degrading organic pollutants in water through advanced oxidation processes: a review. *Water Res* 132:177–189
39. Miao W, Liu Y, Wang D, Du N, Ye Z, Hou Y, Mao S, Ostrikov KK (2021) The role of Fe-N<sub>x</sub> single-atom catalytic sites in peroxymonosulfate activation: formation of surface-activated complex and non-radical pathways. *Chem Eng J* 423:130250
40. Miklos DB, Remy C, Jekel M, Linden KG, Drewes JE, Hübner U (2018) Evaluation of advanced oxidation processes for water and wastewater treatment—a critical review. *Water Res* 139:118–131
41. Myers RL (2007) The 100 most important chemical compounds: a reference guide. ABC-CLIO
42. Neyens E, Baeyens J (2003) A review of classic Fenton's peroxidation as an advanced oxidation technique. *J Hazard Mater* 98(1–3):33–50
43. Oh W-D, Dong Z, Lim T-T (2016) Generation of sulfate radical through heterogeneous catalysis for organic contaminants removal: current development, challenges and prospects. *Appl Catal B* 194:169–201
44. Ohyama J, Abe D, Hirayama A, Iwai H, Tsuchimura Y, Sakamoto K, Irikura M, Nakamura Y, Yoshida H, Machida M (2022) Selective oxidation of methane to formaldehyde over a silica-supported cobalt single-atom catalyst. *J Phys Chem C* 126(4):1785–1792
45. Peng X, Wu J, Zhao Z, Wang X, Dai H, Wei Y, Xu G, Hu F (2022) Activation of peroxymonosulfate by single atom Co-NC catalysts for high-efficient removal of chloroquine phosphate via non-radical pathways: electron-transfer mechanism. *Chem Eng J* 429:132245
46. Peng X, Wu J, Zhao Z, Wang X, Dai H, Xu L, Xu G, Jian Y, Hu F (2022) Activation of peroxymonosulfate by single-atom Fe-g-C<sub>3</sub>N<sub>4</sub> catalysts for high efficiency degradation of tetracycline via nonradical pathways: Role of high-valent iron-oxo species and Fe–N<sub>x</sub> sites. *Chem Eng J* 427:130803
47. Qian K, Chen H, Li W, Ao Z, Wu Y, Guan X (2021) Single-atom Fe catalyst outperforms its homogeneous counterpart for activating peroxymonosulfate to achieve effective degradation of organic contaminants. *Environ Sci Technol* 55(10):7034–7043
48. Qiao B, Wang A, Yang X, Allard LF, Jiang Z, Cui Y, Liu J, Li J, Zhang T (2011) Single-atom catalysis of CO oxidation using Pt 1/FeO<sub>x</sub>. *Nat Chem* 3(8):634–641
49. Qi Y, Li J, Zhang Y, Cao Q, Si Y, Wu Z, Akram M, Xu X (2021) Novel lignin-based single atom catalysts as peroxymonosulfate activator for pollutants degradation: Role of single cobalt and electron transfer pathway. *Appl Catal B* 286:119910
50. Rivera-Cárcamo C, Serp P (2018) Single atom catalysts on carbon-based materials. *Chem-CatChem* 10(22):5058–5091
51. Rong X, Wang H, Lu X, Si R, Lu T (2020) Controlled synthesis of a vacancy-defect single-atom catalyst for boosting CO<sub>2</sub> electroreduction. *Angew Chem* 132(5):1977–1981
52. Ruta V, Sivo A, Bonetti L, Bajada MA, Vilé G (2022) Structural effects of metal single-atom catalysts for enhanced photocatalytic degradation of gemfibrozil. *ACS Appl Nano Mat* 5(10):14520–14528
53. Shang Y, Duan X, Wang S, Yue Q, Gao B, Xu X (2021) Carbon-based single atom catalyst: synthesis, characterization. DFT calculations. *Chinese Chem Lett*

54. Shang Y, Xu X, Gao B, Wang S, Duan X (2021) Single-atom catalysis in advanced oxidation processes for environmental remediation. *Chem Soc Rev*
55. Shrestha S, Wang B, Dutta P (2020) Nanoparticle processing: understanding and controlling aggregation. *Adv Coll Interface Sci* 279:102162
56. Sohlberg K, Pennycook TJ, Zhou W, Pennycook SJ (2015) Insights into the physical chemistry of materials from advances in HAADF-STEM. *Phys Chem Chem Phys* 17(6):3982–4006
57. Song J, Bazant MZ (2012) Effects of nanoparticle geometry and size distribution on diffusion impedance of battery electrodes. *J Electrochem Soc* 160(1):A15
58. Stambula S, Gauquelin N, Bugnet M, Gorantla S, Turner S, Sun S, Liu J, Zhang G, Sun X, Botton GA (2014) Chemical structure of nitrogen-doped graphene with single platinum atoms and atomic clusters as a platform for the PEMFC electrode. *J Phys Chem C* 118(8):3890–3900
59. Tang J, Tang D (2015) Non-enzymatic electrochemical immunoassay using noble metal nanoparticles: a review. *Microchim Acta* 182(13):2077–2089
60. Tong T, Zhu B, Jiang C, Cheng B, Yu J (2018) Mechanistic insight into the enhanced photocatalytic activity of single-atom Pt, Pd or Au-embedded g-C<sub>3</sub>N<sub>4</sub>. *Appl Surf Sci* 433:1175–1183
61. Vasquez-Medrano R, Prato-Garcia D, Vedrenne M (2018) Chapter 4—Ferrioxalate-mediated processes. In: Ameta SC, Ameta R (eds) *Advanced oxidation processes for waste water treatment*. Academic Press, pp 89–113. <https://doi.org/10.1016/B978-0-12-810499-6.00004-8>
62. Wang J, Wang S (2018) Activation of persulfate (PS) and peroxymonosulfate (PMS) and application for the degradation of emerging contaminants. *Chem Eng J* 334:1502–1517
63. Wang S, Wang J (2023) Single atom cobalt catalyst derived from co-pyrolysis of vitamin B12 and graphitic carbon nitride for PMS activation to degrade emerging pollutants. *Appl Catal B* 321:122051
64. Wang L, Zhang W, Wang S, Gao Z, Luo Z, Wang X, Zeng R, Li A, Li H, Wang M (2016) Atomic-level insights in optimizing reaction paths for hydroformylation reaction over Rh/CoO single-atom catalyst. *Nat Commun* 7(1):1–8
65. Wang Y, Zhao X, Cao D, Wang Y, Zhu Y (2017) Peroxymonosulfate enhanced visible light photocatalytic degradation bisphenol A by single-atom dispersed Ag mesoporous g-C<sub>3</sub>N<sub>4</sub> hybrid. *Appl Catal B* 211:79–88
66. Wang A, Li J, Zhang T (2018) Heterogeneous single-atom catalysis. *Nat Rev Chem* 2(6):65–81
67. Wang F, Wang Y, Feng Y, Zeng Y, Xie Z, Zhang Q, Su Y, Chen P, Liu Y, Yao K (2018) Novel ternary photocatalyst of single atom-dispersed silver and carbon quantum dots co-loaded with ultrathin g-C<sub>3</sub>N<sub>4</sub> for broad spectrum photocatalytic degradation of naproxen. *Appl Catal B* 221:510–520
68. Wang Q, Zhang D, Chen Y, Fu W-F, Lv X-J (2019) Single-atom catalysts for photocatalytic reactions. *ACS Sustain Chem Eng* 7(7):6430–6443
69. Wang C, Kim J, Malgras V, Na J, Lin J, You J, Zhang M, Li J, Yamauchi Y (2019) Metal–organic frameworks and their derived materials: emerging catalysts for a sulfate radicals-based advanced oxidation process in water purification. *Small* 15(16):1900744
70. Wang C, Ren H, Wang Z, Guan Q, Liu Y, Li W (2022) A promising single-atom Co-NC catalyst for efficient CO<sub>2</sub> electroreduction and high-current solar conversion of CO<sub>2</sub> to CO. *Appl Catal B* 304:120958
71. Wang P, Huang C, Gao J, Shi Y, Li H, Yan H, Yan S, Zhang Z (2020) Resveratrol induces SIRT1-Dependent autophagy to prevent H<sub>2</sub>O<sub>2</sub>-Induced oxidative stress and apoptosis in HTR8/SVneo cells. *Placenta* 91:11–18
72. Wei H, Liu X, Wang A, Zhang L, Qiao B, Yang X, Huang Y, Miao S, Liu J, Zhang T (2014) FeOx-supported platinum single-atom and pseudo-single-atom catalysts for chemoselective hydrogenation of functionalized nitroarenes. *Nat Commun* 5(1):1–8
73. Wu X, Kim J-H (2022) Outlook on single atom catalysts for persulfate-based advanced oxidation. *ACS ES&T Engineering* 2(10):1776–1796
74. Xiong Z, Jiang Y, Wu Z, Yao G, Lai B (2021) Synthesis strategies and emerging mechanisms of metal-organic frameworks for sulfate radical-based advanced oxidation process: a review. *Chem Eng J* 421:127863

75. Xu L, Fu B, Sun Y, Jin P, Bai X, Jin X, Shi X, Wang Y, Nie S (2020) Degradation of organic pollutants by Fe/N co-doped biochar via peroxymonosulfate activation: Synthesis, performance, mechanism and its potential for practical application. *Chem Eng J* 400:125870
76. Xu J, Zheng X, Feng Z, Lu Z, Zhang Z, Huang W, Li Y, Vuckovic D, Li Y, Dai S (2021) Organic wastewater treatment by a single-atom catalyst and electrolytically produced H<sub>2</sub>O<sub>2</sub>. *Nat Sustain* 4(3):233–241
77. Xue Z-H, Luan D, Zhang H, Lou XWD (2022) Single-atom catalysts for photocatalytic energy conversion. *Joule*
78. Yang T, Fan S, Li Y, Zhou Q (2021) Fe-N/C single-atom catalysts with high density of Fe-N<sub>x</sub> sites toward peroxymonosulfate activation for high-efficient oxidation of bisphenol A: electron-transfer mechanism. *Chem Eng J* 419:129590
79. Yang W, Hong P, Yang D, Yang Y, Wu Z, Xie C, He J, Zhang K, Kong L, Liu J (2021) Enhanced Fenton-like degradation of sulfadiazine by single atom iron materials fixed on nitrogen-doped porous carbon. *J Colloid Interf Sci* 597:56–65. <https://doi.org/10.1016/j.jcis.2021.03.168>
80. Yano J, Yachandra VK (2009) X-ray absorption spectroscopy. *Photosynth Res* 102(2):241–254
81. Yuan Y, Zhao D, Li J, Wu F, Brigante M, Mailhot G (2018) Rapid oxidation of paracetamol by Cobalt (II) catalyzed sulfite at alkaline pH. *Catal Today* 313:155–160
82. Zeng T, Li S, Hua J, He Z, Zhang X, Feng H, Song S (2018) Synergistically enhancing Fenton-like degradation of organics by in situ transformation from Fe<sub>3</sub>O<sub>4</sub> microspheres to mesoporous Fe, N-dual doped carbon. *Sci Total Environ* 645:550–559
83. Zhang Q, Zhang X, Wang J, Wang C (2020) Graphene-supported single-atom catalysts and applications in electrocatalysis. *Nanotech* 32(3):032001
84. Zhang L, Jiang X, Zhong Z, Tian L, Sun Q, Cui Y, Lu X, Zou J, Luo S (2021) Carbon nitride supported high-loading Fe single-atom catalyst for activation of peroxymonosulfate to generate 1O<sub>2</sub> with 100% selectivity. *Angew Chem Int Ed* 60(40):21751–21755
85. Zhang N, Zhang X, Tao L, Jiang P, Ye C, Lin R, Huang Z, Li A, Pang D, Yan H (2021) Silver single-atom catalyst for efficient electrochemical CO<sub>2</sub> reduction synthesized from thermal transformation and surface reconstruction. *Angew Chem Int Ed* 60(11):6170–6176
86. Zhao C, Xiong C, Liu X, Qiao M, Li Z, Yuan T, Wang J, Qu Y, Wang X, Zhou F (2019) Unraveling the enzyme-like activity of heterogeneous single atom catalyst. *Chem Commun* 55(16):2285–2288
87. Zhou Z, Li M, Kuai C, Zhang Y, Smith VF, Lin F, Aiello A, Durkin DP, Chen H, Shuai D (2021) Fe-based single-atom catalysis for oxidizing contaminants of emerging concern by activating peroxides. *J Hazard Mater* 418:126294
88. Zhu S, Li X, Kang J, Duan X, Wang S (2018) Persulfate activation on crystallographic manganese oxides: mechanism of singlet oxygen evolution for nonradical selective degradation of aqueous contaminants. *Environ Sci Technol* 53(1):307–315